

Estimation of broadband emissivity (8-12um) from ASTER data by using RM-NN

K. B. Mao,^{1,2,7} Y. Ma,^{3,8} X. Y. Shen,⁴ B. P. Li,⁵ C. Y. Li,² and Z. L. Li⁶

¹Key Laboratory of Agri-informatics, MOA, and Hulunber Grassland Ecosystem Observation and Research Station, Institute of Agricultural Resources and Regional Planning, Chinese Academy of Agricultural Sciences, Beijing 100081, China

²Northwest Land and Resources Research Center, Shaanxi Normal University, Xi'an 710062, China

³A-World Consulting, Hong Kong Logistics Association, Hong Kong 999077, China

⁴Institution of Remote Sensing and Geographical Information System, Peking University, Beijing 100871, China

⁵Department of Electronic Engineering, The Chinese University of Hong Kong, Hong Kong SAR, China

⁶Laboratoire des Sciences de l'Image, de l'Informatique et de la Télédétection/Ecole Nationale Supérieure de Physique de Strasbourg, UMR 7005, Illkirch, France

⁷maokebiao@126.com

⁸maying_helen@163.com

Abstract: Land surface window emissivity is a key parameter for estimating the longwave radiative budget. The combined radiative transfer model (RM) with neural network (NN) algorithm is utilized to directly estimate the window (8–12 um) emissivity from the brightness temperature of the Advanced Spaceborne Thermal Emission and Reflection Radiometer (ASTER) with 90 m spatial resolution. Although the estimation accuracy is very high when the broadband emissivity is estimated from AST05 (ASTER Standard Data Product) by using regression method, the accuracy of AST05 is about ± 0.015 for 86 spectra which is determined by the atmosphere correction for ASTER 1B data. The MODTRAN 4 is used to simulate the process of radiance transfer, and the broadband emissivity is directly estimated from the brightness temperature of ASTER 1B data at satellite. The comparison analysis indicates that the RM-NN is more competent to estimate broadband emissivity than other method when the brightness temperatures of band 11, 12, 13, 14 are made as input nodes of dynamic neural network. The estimation average accuracy is about 0.009, and the estimation results are not sensitive to instrument noise. The RM-NN is applied to extract broadband emissivity from an image of ASTER 1B data in China, and the comparison against a classification based multiple bands with 15 m spatial resolution shows that the estimation results from RM-NN are very good.

©2012 Optical Society of America

OCIS codes: (010.5630) Radiometry; (010.0280) Remote sensing and sensor; (280.4991) Passive remote sensing; (010.7340) Emissivity; (010.3920) Metrology; (100.3190) Inverse problem.

References and links

1. A. C. Wilber, D. P. Kratz, and S. K. Gupta, "Surface emissivity maps for use in satellite retrievals of longwave radiation," NASA/TP-1999-209362, 30 (1999).
2. C. Prabhakara and G. Dalu, "Remote sensing of the surface emissivity at 9 um over the globe," J. Geophys. Res. **81**(21), 3719–3724 (1976).
3. E. F. Wood, D. P. Lettenmaier, L. Xu, D. Lohmann, A. Boone, S. Chang, F. Chen, Y. Dai, R. E. Dickinson, Q. Duan, M. Ek, Y. M. Gusev, F. Habets, P. Irannejad, R. Koster, K. E. Mitchel, O. N. Nasonova, J. Noilhan, J. Schaake, A. Schlosser, Y. Shao, A. B. Shmakin, D. Verseghy, K. Warrach, P. Wetzel, Y. Xue, Z. L. Yang, and Q. Zeng, "The project for intercomparison of land-surface parameterization scheme (PILPS) Phase 2(c) Red-Arkansas River basin experiment: I. Experiment description and summary intercomparisons," Global Planet. Change **19**, 115–135 (1998).

4. C. Blondin, *Parameterization of Land-Surface Processes in Numerical Weather Prediction, in Land Surface Evaporation*, T. J. Schmugge and J. Andre, eds. (Springer-Verlag, New York, 1991) pp. 31–54.
 5. K. Mao, J. Shi, H. Tang, Z. Li, X. Wang, and K. Chen, "A Neural network technique for separating and surface emissivity and temperature from ASTER imagery," *IEEE Trans. Geosci. Rem. Sens.* **46**(1), 200–208 (2008).
 6. K. Ogawa, T. Schmugge, and F. Jacob, "Estimation of land surface window (8–12 μm) emissivity from multi-spectral thermal infrared remote sensing — A case study in a part of Sahara Desert," *Geophys. Res. Lett.* **30**(2), 1067 (2003), doi:10.1029/2002GL016354.
 7. A. Gillespie, S. Rokugawa, T. Matsunaga, J. S. Cothren, S. Hook, and A. B. Kahle, "A temperature and emissivity separation algorithm for advanced spaceborne thermal emission and reflection radiometer (ASTER) images," *IEEE Trans. Geosci. Rem. Sens.* **36**(4), 1113–1126 (1998).
 8. J. W. Salisbury and D. M. D'Aria, "Emissivity of terrestrial materials in the 8–14 mm atmospheric window," *Remote Sens. Environ.* **42**(2), 83–106 (1992).
 9. W. C. Snyder, Z. Wan, Y. Zhang, and Y. Feng, "Thermal infrared (3–14mm) bi-directional reflectance measurement of sands and soils," *Remote Sens. Environ.* **60**(1), 101–109 (1997).
 10. D. E. Bowker, R. E. Davis, D. L. Myrick, K. Stacy, and W. T. Jones, "Spectral reflectances of natural targets for use in remote sensing studies," NASA Reference Pub. **1139** (1985).
 11. Y. C. Tzeng, K. S. Chen, W. L. Kao, and A. K. Fung, "A dynamic learning neural network for remote sensing applications," *IEEE Trans. Geosci. Rem. Sens.* **32**(5), 1096–1102 (1994).
 12. K. Mao, H. Tang, X. Wang, Q. Zhou, and D. Wang, "Near-surface air temperature estimation from ASTER data based on neural network algorithm," *Int. J. Remote Sens.* **29**(20), 6021–6028 (2008).
 13. K. Mao, S. Li, D. Wang, L. Zhang, H. Tang, X. Wang, and Z. Li, "Retrieval of land surface temperature and emissivity from ASTER1B data using dynamic learning neural Network," *Int. J. Remote Sens.* **32**(19), 5413–5423 (2011).
 14. A. Berk, L. S. Bemstein, and D. C. Robertson, "MODTRAN: a moderate resolution model for LOWTRAN," Burlington, MA, Spectral Science, Inc. Rep. AFGL-TR-87-0220 (1987).
-

1. Introduction

In recent years, the study of Earth's radiation has made the remote sensing of broadband emissivity as an important issue because of the extensive requirement of broadband emissivity information for estimation of energy balance. The surface emissivity at surface window wavelengths is one of critical parameters in earth-atmosphere system radiation budget studies. An empirical emissivity is used in many numerical weather predictions and land surface energy balance model. Although it is very difficult to obtain the emissivity, many efforts have been devoted to the establishment of methodology for estimating broadband emissivity from remote sensing data. The broadband emissivity is obtained by classifying data with corresponding spectral libraries [1–4]. The advantage of this method is relative easy to obtain the broadband emissivity, but it cannot reflect the dynamic change of emissivity with the change of environment and the time. As we all know that the vegetation is changed in different season, especially for crops.

The ASTER is an imaging instrument aboard the Terra satellite, which was launched in December 1999 as part of the National Aeronautics and Space Administration's (NASA's) Earth Observing System (EOS). ASTER has 15 bands, which cover the visible, near-infrared, short-wave infrared, and thermal infrared regions, and the spatial resolution is from 15 to 90 m [5]. Ogawa *et al.* [6] used regression method to estimate the broadband (8–12 μm) emissivity from AST05 data, and the error of broadband emissivity is about ± 0.005 for simulation data. AST05 is five thermal infrared channels emissivity product which are produced by using Temperature-Emissivity Separation (TES) algorithm [7]. Based on numerical simulation for 86 laboratory reflectance spectra of rocks, soils, vegetation, snow and water, the errors of emissivities estimated by TES algorithm are within about ± 0.015 under given that the atmosphere correction is very good. That means that the error of broadband emissivity is about ± 0.02 for 86 laboratory reflectance spectra in the ideal situation. As we all know that, the number of reflectance spectra is more than 86, and the accuracy of atmosphere correction cannot be guaranteed because we cannot obtain the water vapor content with same resolution. So the estimation accuracy needs to be improved further.

In Section 2 of this paper we will present why and how to improve estimation accuracy by using a combined radiative transfer model (RM) neural network (NN) algorithm to

estimate broadband emissivity from ASTER 1B data. In Section 3 the sensitivity and application analysis will be made. Finally, conclusions are given in Section 4.

2. RM-NN Methods for estimating broadband emissivity

The broadband emissivity (ε_{8-12}) between 8 and 12um is defined as Eq. (1) [6].

$$\varepsilon_{8-12} = \frac{\int_{\lambda=8}^{\lambda=12} \varepsilon(\lambda)B(\lambda,T)d\lambda}{\int_{\lambda=8}^{\lambda=12} B(\lambda,T)d\lambda}, \quad (1)$$

where $\varepsilon(\lambda)$ is spectral emissivity at the wavelength λ , $B(\lambda,T)$ is Planck function, and T is surface temperature. Due to the influence of atmosphere, just the window band emissivity at remote sensor can be obtained. Ogawa *et al.* (2003) proposed a regression method for estimating broadband emissivity (ε_{8-12}) by using five thermal infrared bands. The computation expression is as Eq. (2):

$$\varepsilon_{8-12} = 0.014\varepsilon_{10} + 0.145\varepsilon_{11} + 0.241\varepsilon_{12} + 0.467\varepsilon_{13} + 0.004\varepsilon_{14} + 0.128. \quad (2)$$

257 spectra are collected from ASTER spectral library [8, 9], and 49 spectra are selected from [10]. We assume that $T = 300$ K in this analysis, and the Eq. (1) is used to compute the broadband emissivity between 8 and 12um. The comparison between truth emissivity and emissivity estimated by Eq. (2) is like Fig. 1. The average error of emissivity is under 0.006.

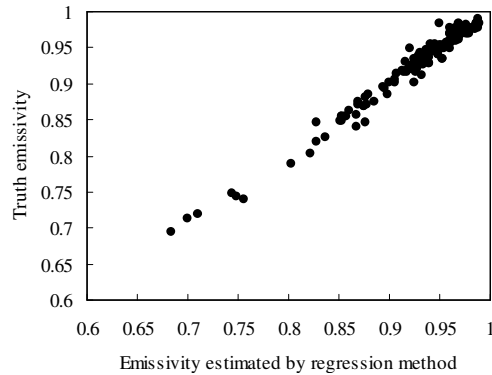


Fig. 1. The comparison between truth emissivity and emissivity estimated by regression method.

Although the accuracy of the method mentioned above is very high, it is determined by the accuracy of the each thermal band emissivity which is retrieved from the brightness temperature at satellite. The errors of emissivities estimated by TES algorithm are within about ± 0.015 for 86 spectra under given that the atmosphere correction is very good [7]. So the accuracy is about ± 0.02 in ideal conditions.

Many studies have proved the inherent capabilities of the NN to perform classification, function approximation, optimization computation, and self-learning. The complicated relationships between geophysical parameters determine that the NN is one of the best ways to solve the complex inverse problem [11–13]. Mao et al [5, 13] made much analysis and proved that the accuracy can be improved if we use the optimized algorithm neural network to retrieve land surface temperature and emissivity from ASTER data. So we make an analysis for estimating broadband emissivity from brightness temperature at satellite. The MODTRAN4 [14] is used to simulate the process of radiance transfer. We use every band

emissivity in bands 10–14 as input parameters for MODTRAN4. The range of LST is from 270 to 320 K with step size 10 K, and the near surface air temperature (at 2 m height) is arbitrarily assumed from 273 to 310 K with step sizes of 3 and 5 K. The range of atmospheric water vapor content is from 0.2 to 4 g cm⁻² with a step size of 0.5 g cm⁻², and the atmospheric profile of midlatitude summer is used for simulation. These simulation data sets are viewed as reference data from a known ground truth. We divide the simulation data randomly into two parts. The first part 8431 sets are made as training data, and the other 2253 sets are testing data. The brightness temperatures of five thermal bands are made as five input nodes, and the broadband emissivity is made as output node. In this study, we select the dynamic learning neural network (DL) [11] to estimate broadband emissivity. The DL is different from a general neural network in that it uses the Kalman filtering algorithm to increase the convergence rate in the learning stage and enhance separately the ability for the highly nonlinear boundaries problem [11]. The initial neural network weights are set to be small random numbers (–1, 1). The Kalman filtering process is a recursive mean square estimation procedure. Each updated estimate of neural network weight is computed from the previous estimate and the new input data. The weights connected to each output node can be updated independently. Part of test results is as Table 1. The average error of broadband emissivity is under 0.012 when two hidden layers are with 500 nodes each.

Table 1. The Estimated Error from Brightness Temperatures in Bands 10-14 at Satellite

Hidden nodes	Emissivity			
	Average Error	Average Error (Percent)	R	SD
100-100	0.0264	0.0245	0.428	0.041
200-200	0.023	0.0238	0.465	0.0334
300-300	0.0221	0.0228	0.482	0.029
400-400	0.0157	0.0203	0.576	0.027
500-500	0.0113	0.0116	0.794	0.009
600-600	0.0126	0.0129	0.726	0.0111
700-700	0.0138	0.0141	0.69	0.0134
800-800	0.0148	0.0154	0.64	0.0211

^aR: Correlation coefficient; SD: Standard deviation of the fit.

The band 10 has some interference for estimation accuracy because transmittance of band 10 is very low. So we make four brightness temperatures of band 11-14 as four input nodes, and broadband emissivity is made as output node. Part of test results is as Table 2. The average error of broadband emissivity is about 0.009 when two hidden layers are with 700 nodes each and the distribution of average error is like Fig. 2. The accuracy is improved when we use the brightness temperatures of bands 11-14 as input nodes. This method overcomes the difficulty of atmosphere correction in regression method, which simplifies the computation process and improves estimation accuracy. Shown from the hidden nodes in Table 1 and Table 2, the process of radiance transfer is very complicated.

Table 2. The Estimated Error from Brightness Temperature in Bands 11-14 at Satellite

Hidden nodes	Emissivity		R	SD
	Average Error	Average Error (Percent)		
100-100	0.0127	0.0131	0.733	0.0143
200-200	0.0125	0.0129	0.733	0.0131
300-300	0.0117	0.0121	0.752	0.012
400-400	0.0111	0.0114	0.766	0.01
500-500	0.0101	0.0114	0.786	0.011
600-600	0.0097	0.011	0.791	0.0099
700-700	0.0091	0.0095	0.837	0.0081
800-800	0.0094	0.0098	0.814	0.0092

^aR: Correlation coefficient; SD: Standard deviation of the fit.

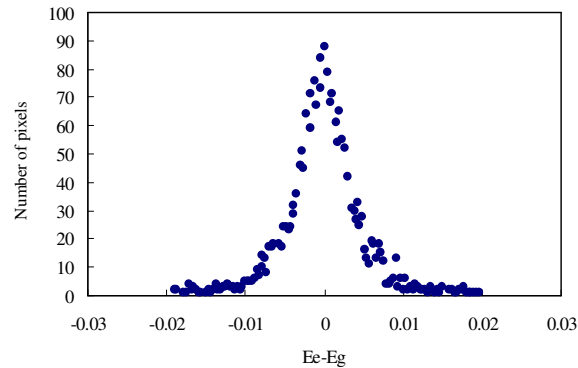


Fig. 2. . The distribution of average error.

3. Sensitivity and application analysis

The broadband emissivity is directly estimated from brightness temperatures at satellite, so the sensitivity is mainly determined by Sensor. The base line performance requirements of bands 10-14 is like first three columns in Table 3. The estimation error of broadband emissivity is in fourth column in Table 3. The brightness temperatures of bands 11-14 at sensor are higher 240 K in most conditions, and estimation error of broad emissivity is less than 0.016. Thus, the estimation results are not sensitive for instrument noise.

Table 3. The Sensitivity Analysis for Algorithm

Spectral Coverage	Rang of Bright Temperature at Satellite	Absolute Temperature Accuracy	Estimation Error of Broadband Emissivity
8.3- 11.65 μm	200 - 240 K	≤ 3 K	0.016
	240 - 270 K	≤ 2 K	0.0013
	270 - 340 K	≤ 1 K	0.0095
	340 - 370 K	≤ 2 K	0.001

In order to give an application example, we use this DL neural network, which has been trained above to estimate the broadband emissivity from ASTER 1B data. The inputs of neural network are brightness temperature (T_i , $i = 11/12/13/14$), and the output is the broadband emissivity. We select an ASTER image in Heilongjiang province, China (09/09/2005) as research region. Figure 3(a) is the classification map by using band 1, 2, 3 with 15 m spatial resolution. Figure 3(b) is the broadband emissivity estimated by RM-NN with 90 m spatial resolution. Shown from Fig. 3, the broad emissivity is almost consistent with the classification map.

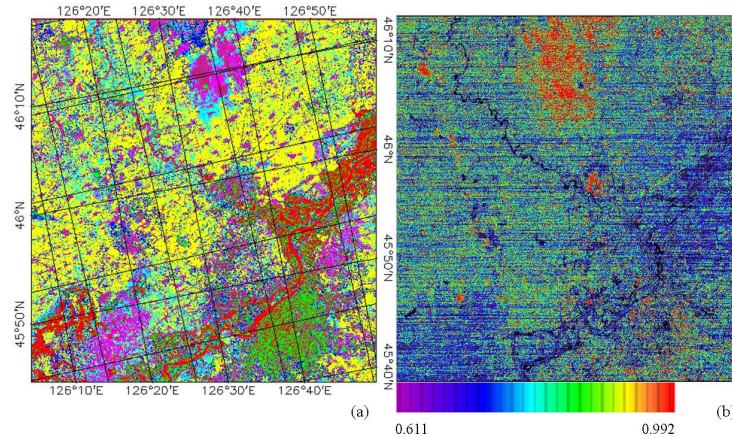


Fig. 3. (a) Classification map (band 1, 2, 3), (b) broadband emissivity.

4. Conclusion

The regression method for estimating broadband emissivity from ASTER data is suitable for 86 spectra, and deviation is relative large because some spectral curve is very different from them. The other disadvantage is that the accuracy is determined of the AST05 product, which is influenced by atmosphere correction. It is very difficult to obtain the atmosphere parameters to eliminate the influence of the atmosphere, which make this method complicated. The accuracy is about ± 0.02 in ideal conditions.

We utilize MODTRAN4 to simulate data to train and test neural networks. The test results indicate that RM-NN is very robust. The estimated accuracy by using brightness temperature of band 11-14 is higher than by using brightness temperatures of band 10-14 as input nodes of neural network because the transmittance of band 10 is very low. The accuracy is about 0.009 when the number of hidden layers is two and the number of hidden nodes is 700–700. The sensitivity analysis indicates that the noise of instrument has not much influence for the estimation error. The trained neural network (DL) is used to estimate broadband emissivity from the ASTER 1B data. The comparison analyses indicate that the estimation results by RM-NN is almost consistent with classification map with 15 m spatial resolution. The main purpose of this study proves that RM-NN is competent for estimating broadband emissivity, and simplifies the estimation process and improves the estimation accuracy. We will do further application analysis that will be reported in future and will make RM-NN more robust and suitable for more conditions.

Acknowledgments

This work was supported by 973 Program (No. 2010CB951503); the National Natural Science Foundation of China (No. 40930101).